

Planning Energy Storage and Photovoltaic Panels for Demand Response with Heating Ventilation and Air Conditioning Systems

Mohammed Alhaider, Lingling Fan*

Abstract—The objective of this engineering problem is to determine the size of a battery energy storage system (BESS) and number of photovoltaic (PV) panels to be installed in a building with Heating Ventilation and Air Conditioning systems (HVACs) as the main load. The building is connected to the power grid where electricity price is varying at different hours. This engineering problem is formulated as an optimization problem with a goal to achieve minimum installation cost and operation cost while satisfying room temperature requirements. Stochastic PV outputs are taken into consideration as well. The mathematical problem formulated is a large-scale mixed integer linear programming (MILP) problem. To improve the solving speed, two Benders Decomposition strategies are applied to solve this stochastic MILP problem. The optimization problem will lead to the battery energy capacity, power limit, number of PV to be installed, as well as the on/off status of HVACs over eight hours. The contribution of this paper is the implementation of Benders decomposition methods to reduce the computation complexity. Parallel computing structure and maximum feasible subsystem cut generation strategy have been exploited and implemented in this research.

Index Terms—HVAC, Battery, Demand Response, Bender Decomposition

I. INTRODUCTION

Demand response at the load side attracts interest to the industry. With peak demand reduced through demand response, construction of new power plants can be delayed [1]. Residential and commercial building are one of the major loads during peak hours. According to [2], 40% to 60% of peak loads are commercial and residential building loads.

HVACs are the main component of the building loads. Due to its thermal storage capability, HVACs have been considered for demand response [3]. Many buildings have roof tops with PV panels installed to harvest solar energy. These PV panels can be used to power up the HVAC units. Due to PV power's intermittent nature, BESS are often time used along with PV panels. The BESS can mitigate the fluctuation of renewable output. Further, the output of BESS is controllable. Hence the integrated system with PV, BESS and the building can be treated as a controllable load to realize demand response, e.g., peak shaving, valley filling, and responding to time-varying electricity prices [4].

A. Mathematic programming problem formulation

This paper deals with planning BSEE and PV panels for a building with HVACs as the main load. Sizing a BSEE to accommodate varying load and/or energy sources has been investigated in the literature [5]–[13]. Based on the time frame of cycling requirements, the applications of battery storage can be classified into real-time, intra-hour, intra-day and slow varying [13]. For example, the frequency of cycling for intra-day applications is at about every several hours. That is, a battery will be charged and discharge once per several hours. The applications in [6]–[12] are all related to intra-day applications. Several methods have been used in determining battery size. In [13], battery size is determined by cycling requirements. In [5], probabilistic methods are used to determine the size of a battery. In [10], size is determined using risk analysis method. [8] determines the size of a BESS through time-domain simulation. A major portion of the literature, however, takes the mathematical programming problem formulation approach, e.g., [6], [9], [11], [12]. Further, stochastic programming approach is adopted in [9].

In this paper, we further consider HVAC load in the BESS and PV sizing problem. In addition, the integrated BESS, PV and HVAC system will participate in demand response. Therefore, the integrated system will react based on the electricity price.

An HVAC system's control inputs include input air pressure and temperature setting. Sophisticated dynamic models with air pressure and temperature setting as the inputs have been adopted in thermal energy storage studies [14], [15]. In electric power planning and operation studies, a simplified thermal dynamic model of first-order is usually adopted, e.g., [16]–[18], where the HVAC control input is simplified as on/off status. The on/off status is determined simply by a price comparison rule in [16] while in [17], [18], mixed integer programming (MIP) problems are formulated for the decision making process and the problems are solved by heuristic methods. In [19], HVAC loads are modeled as continuously controllable loads. Such a model is overly optimistic and does not capture HVAC's operation characteristics. In this research, the first-order thermodynamic model with on/off input is adopted.

In addition to HVAC modeling, stochastic PV output should also be modeled. Uncertainty is usually modeled using stochastic scenarios, e.g., [20]–[22]. To have a reasonable representation of stochastic, numerous scenarios are usually created. This leads to a large-scale optimization problems.

M. Alhaider and L. Fan are with Department of Electrical Engineering, University of South Florida, Tampa FL USA 33620. Email: linglingfan@usf.edu.

B. Large-scale MILP problem solving techniques

With HVAC on/off status considered, binary variables are introduced into the programming problems and large-scale MILP problems are expected. Solving large-scale MILP problems is a challenging task. Computing time increases quickly when the dimension of the problem increases if commercial solvers (CPLEX [23] or Gurobi [24]) are adopted.

Alternatively, heuristic methods, e.g., genetic algorithm, have been adopted in the literature for large-scale MILP problems [19]. Heuristic methods do not guarantee a global optimum. They have the similar scalability issues as commercial solvers.

A better approach is to develop customized algorithm to be used along with commercial solvers. For example, branching and bound solving strategy is applied in [25] for task scheduling while Benders decomposition is applied in [26] for unit commitment. Among the two methods, Benders decomposition is a well-known efficient algorithm to handle large-scale MIP problems. Applications of Benders decomposition are plenty in power systems, e.g., unit commitment considering wind [26], optimal power flow considering uncertainty [27], transmission planning considering wind [28].

Benders decomposition technique separates decision variables into two categories and forms a master problem with one subset of decision variables, one or multiple subproblems with the rest set of the decision variables. The subproblems are solved and valid inequality constraints are created and added to the master problem. Through iterations, convergence will be achieved and a global solution will be found for a MILP problem. Interested readers can find a tutorial on Bender's decomposition in [29].

C. Our contribution

Our contribution is twofold. Firstly, a stochastic programming problem is formulated to emulate 8-hour demand response operation of PV, battery and HVAC. Secondly, this paper presents the solving technique for the proposed large-scale stochastic programming problem using Benders decomposition technique. Such a large-scale problem cannot be solved by an off-shelf commercial MIP solver, e.g., CPLEX, after 24 hours. On the other hand, with the proposed solving technique, the numerical simulation has been performed on a 3.4-GHz based processor with 8GB of RAM and the maximum execution time is 35 minutes.

Compared to [30], where a MILP optimization problem is formulated for this engineer problem and Benders decomposition is adopted to have one master problem and one subproblem, the current paper refines the Bender's decomposition technique and proposes another Bender's decomposition formulation with one master problem and multiple subproblems. Both formulations are presented in this paper for comparison. The second formulation has a parallel computing structure and can handle even more stochastic scenarios. Further, maximum feasible subsystem cut generation technique are exploited and implemented to advance the computing. There two variations of Benders decomposition are examined in the case studies.

The rest of the paper is organized as follows. Section

II presents the HVAC model. Section III presents the optimization problem formulation. Section IV presents the two variations of Benders decomposition techniques. Section V presents case studies and Section VI concludes the paper.

II. THERMAL DYNAMICS MODELS OF AN HVAC UNIT

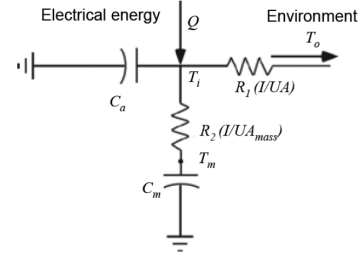


Fig. 1: The HVAC model.

The simplified first-order thermal dynamic model [16]–[18] is shown in Fig. 1 and is equivalent to an RC circuit. When the HVAC is turned OFF, the room temperature at time is described by

$$T_{\text{room}}^{j+1} = T_o^{j+1} - (T_o^{j+1} - T_{\text{room}}^j)e^{-\Delta t/RC}. \quad (1)$$

where j denotes j th period, Δt is the length of each time period. C denotes the equivalent heat capacity (Btu/F), R denotes the equivalent thermal resistance (F/W), and T_o^j denotes ambient temperature (F) at j th period, Q denotes heat rate for HVAC unit (Btu/hr or W), and T_{room} denotes air temperature inside the house (F).

When the cooler is turned ON, the room temperature at time is described by

$$T_{\text{room}}^{j+1} = T_o^{j+1} + QR - (T_o^{j+1} + QR - T_{\text{room}}^j)e^{-\Delta t/RC} \quad (2)$$

(1) and (2) will be combined into one thermal constraint through a binary variable W^j (1: the cooler is on; 0: the cooler is off).

$$T_{\text{room}}^{j+1} = T_o^{j+1} + W^j QR - (T_o^{j+1} + W^j QR - T_{\text{room}}^j)e^{-\frac{\Delta t}{RC}}$$

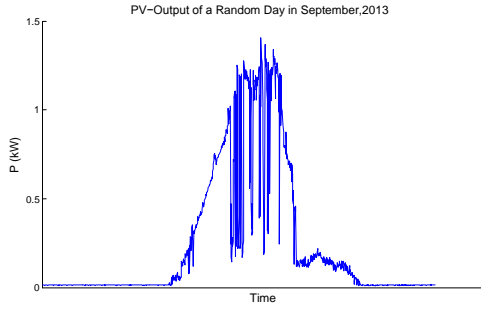
III. OPTIMIZATION PROBLEM FORMULATION

A. Modeling Uncertainty of PV Output

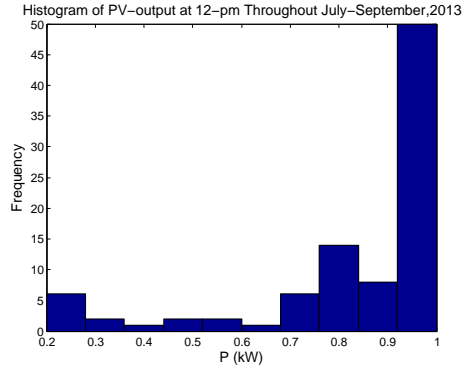
Scenarios of PV output can be developed based on real-world data collected from the PV panels that are installed at the St. Pete campus of University of South Florida. PV output of a random day is shown in Fig. 2a.

PV power data are collected every minute. For each hour span, the power data are averaged to find the hourly PV power. The hourly PV power data are categorized into different levels.

For a whole month's PV data, for each hour, the occurring frequency of each power level would be calibrated. Fig. 2b shows an example of the histogram for the PV power at 12 PM. From this histogram, we may create scenarios and assign each scenario with a probability. For example, we consider three power levels (low, medium and high). Approximately 64% of the chance, the PV output occurred between 0.9-1



(a) PV-output of a random day.



(b) Histogram of PV-output at 12 PM based on three months' data.

Fig. 2: PV power characteristics.

kW, approximately 24% of the chance, the PV output occurred between 0.6-0.8 kW, and 12% of the chance that the PV output occurred between 0.2-0.5 kW. This method is applied to the rest of the hours and three different PV output level at each hour for eight hours (from 10 am to 5 pm) with its probability of occurring are listed in Table. I. The rest of the hours are not considered in the study since the PV output for those hours are negligible.

TABLE I: PV output level and probability

Hour	10 am	11 am	12 pm	1 pm	2 pm	3 pm	4pm	5pm
High (kW)	0.90	0.80	0.95	1.20	1.30	0.90	0.80	0.70
Probability	0.75	0.73	0.64	0.71	0.70	0.60	0.75	0.72
Medium (kW)	0.70	0.50	0.80	0.90	1.00	0.60	0.60	0.40
Probability	0.15	0.18	0.24	0.16	0.19	0.35	0.15	0.21
Low (kW)	0.30	0.40	0.20	0.70	0.80	0.40	0.30	0.20
Probability	0.10	0.09	0.12	0.13	0.11	0.05	0.10	0.09

The total number of scenarios that can be created from Table I are 3^8 (6561) scenarios. The probability of each scenario can be evaluated using statistic analysis. Note that PV's hourly outputs at different hours are dependent to each other. In the literature, probability will be evaluated using methods such as Markov Chain, e.g., [31]. Further, PV's output is dependent on weather condition and other factors such as adequate PV installation. A comprehensive study will be needed to assign an accurate probability to each scenario. These work will be conducted in our future research. In this paper, we selected 600 scenarios and assigned a probability to each scenario to have the sum of probabilities equal 1.

B. Optimization Model

The optimization model is developed based on the assumption that there is a BESS to be installed and can be charged and discharged to store energy from the grid or supply the HVAC with power. In addition, there are PV panels with fixed rated power to be installed. The optimization problem is to determine how many PV panels to be installed and what is the best capacity and power rating for the battery given the system has a number of HVAC with thermal constraints to meet for an 8-hour horizon. The 8-hour time span is further divided into 32 horizons with each horizon 15 minutes.

The assumption of the operation is that the HVAC on/off sequence is not stochastic. Rather, the on/off sequence is deterministic. This assumption is realistic as HVAC's on/off sequence is usually fixed ahead of time. On the other hand, the battery's charging/discharging power level, the building's purchased power P_{in} are stochastic scenario based. This is due to the stochastic nature of PV output. The battery power and purchased power level decision are usually determined at real-time.

The following three paragraphs give the decision variables, the objective function and the constraints.

1) Decision Variables:

$$X = \left[C_b \ E_b \ N_{pv} \ P_{in}^{s,j} \ P_b^{s,j} \ W_k^j \right] \quad (3)$$

where:

j denotes j th period, $j \in J = \{1, 2, \dots, 32\}$. 8-hour is considered with each period 15 minutes.

k denotes k th No. of HVAC unit. $k \in K = \{1, 2, 3\}$.

s denotes s th scenario. $s \in S$, where S contains 600 scenarios in the case study.

C_b denotes the power rating of the battery energy system.

E_b denotes the energy rating of the battery energy system.

N_{pv} denotes the number of PV panels to be installed.

$P_{in}^{s,j}$ denotes purchased power at the j -th period of the s th scenario.

W_k^j denotes a binary variable: 1 if the k -th HVAC is on at the j -th period; and 0 otherwise.

$P_b^{s,j}$ denotes the battery discharging power at j -th period of the s -th scenario. A negative value means the battery is charging.

2) *Objective Function*: The objective is to minimize the installation cost of BESS and PV panels, at the same time the expected cost of power purchasing from the main grid.

$$\min \left\{ \beta_1 C_b + \beta_2 E_b + \alpha N_{pv} + \sum_{s \in S} \sum_{j \in J} \rho_s \left(\lambda^j P_{in}^{s,j} \right) \right\} \quad (4)$$

where

β_1 denotes the cost of 1 kW rating of the BESS.

β_2 denotes the cost of 1 kWh rating of the BESS.

α denotes the cost of installation of PV panel.

ρ_s denotes the probability of s -th scenario.

λ^j denotes the energy price at the j th period.

Note the first three components of the objective functions are deterministic and related to the installation cost. The last

component is related to the expected cost over all periods due to power purchasing.

3) *Constraints*: Constraint set (5) describes the room temperature dynamics and ensures that thermostat setting is enabled where the temperature of the room must be greater than the minimum temperature and less than the maximum temperature. This constraint set does not contain probability scenarios since the HVAC operation is assumed to be deterministic for the possible scenarios.

$$\begin{aligned} T_k^{j+1} &= T_o^{j+1} + W_k^j QR - (T_o^{j+1} + W_k^j QR - T_k^j) e^{-\frac{\Delta t}{RC}} \\ T_{\min} &\leq T_k^{j+1} \leq T_{\max} \quad \forall j \in J \end{aligned} \quad (5)$$

Constraint set (6) guarantees that there is enough available power when the HVAC unit is turned on. It also ensures that the purchased power is within the power limits. This set of constraints are scenario-based.

$$\begin{aligned} P_{in}^{s,j} + P_b^{s,j} + N_{pv} P_{PV}^{s,j} &\geq \sum_{i=1}^k W_k^j P_{ac,k} \\ P_{\min} &\leq P_{in}^{s,j} \leq P_{\max} \quad \forall j \in J, \forall k \in K, \forall s \in S \end{aligned} \quad (6)$$

where $P_{ac,k}$ is a fixed power consumption for k -th HVAC.

Note that for the power balance relationship, inequality is adopted instead of equality. We consider that HVAC as the main load and the building may have other loads. The total power generated from PV, purchased from outside and discharged from the battery should at least meet the requirement of the HVAC. Considering that the engineering problem is a planning problem instead of real-time operation problem where power generation has to equal power consumption, this assumption is reasonable.

Constraint set (7) makes sure that at any hour j and any scenario s , the battery charging or discharging does not exceed the battery power rating and the energy at any hour will not exceed the energy limits.

$$\begin{aligned} -C_b &\leq P_b^{s,j} \leq C_b \quad \forall j \in J, \forall s \in S \\ 0 &\leq E_0 - \sum_{i=1}^j P_b^{s,i} \leq E_b \quad \forall j \in J, \forall s \in S \end{aligned} \quad (7)$$

IV. LARGE-SCALE PROBLEM SOLVING USING BENDERS DECOMPOSITION

The optimization problem formulated in Section III is a large-scale problem. The size of the problem increases as the number of scenarios increase. It includes a mixture of integer and continuous variables and would depend on the number of HVAC units, time steps, and scenarios. When 3 HVAC, 32 horizons, and 25 scenarios are considered, the problem has 96 binary variables (related to 3 HVAC units running for 32 time horizons) and one integer variable related to the number of PV. It would also have 99 continuous variables related to the room temperature and two continuous variables related to the battery parameters (C_b and E_b). While all aforementioned variables are independent of the number of scenarios, the rest variables are related scenarios. Those variables include 800 continuous variables (related to the purchased power considering 25

scenarios for 32 time horizons) and 800 continuous variables (related to battery power P_b considering 25 scenarios for 32 time horizons). This formulation is solved using CPLEX in MATLAB and the main challenge here is the very slow computing time (hours).

With 600 scenarios, CPLEX was tested to solve the problem for 24 hours without giving any solution. Therefore, Benders decomposition, an effective method of large-scale MIP problem solving is implemented in this research.

A. Benders Decomposition with A Single Subproblem

The main philosophy is to separate the decision variables into two sets: those related to HVAC, and those not related to HVAC. The first set includes integer variables including W (which denotes HVAC on/off) and the number of PV, as well as the continuous variables (room temperatures). The second set includes the rest of variables including battery power dispatch level, battery power and energy ratings. The second set variables are all continuous. The solving procedure is to fix Set 1 variables and solve the subproblem related to Set 2. With the solved subproblem, we generate a dual cut to reduce the feasible region of the main problem associated with Set 1 variables. The procedure is kept going until convergence.

a) *Step 1*: In this step, we assume that the power and energy ratings of a battery, power demand are all zero. Only the HVAC operation is considered. The master problem is formed and we find its optimal solution as follows.

$$\min_{N_{pv}, W_k^j} Z_{\text{lower}} \quad (8a)$$

$$\text{s.t. } Z_{\text{lower}} \geq \alpha N_{pv} \quad (8b)$$

$$T_k^{j+1} = T_o^{j+1} + W_k^j QR - (T_o^{j+1} + W_k^j QR - T_k^j) e^{-\frac{\Delta t}{RC}} \quad (8c)$$

$$T_{\min} \leq T_k^{j+1} \leq T_{\max} \quad \forall j \in J, k \in K \quad (8d)$$

b) *Step 2*: Step 1 gives the number of PVs and the on/off status of HVAC. We now form the subproblem using the fixed values (\hat{N}_{pv} , \hat{W}_k^j).

The subproblem is to minimize the cost of battery installation and the expected cost for energy purchasing. Constraints related to power balance, purchasing power limits, and battery constraints are included. The subproblem is presented in (9).

$$\min_{\substack{C_b, E_b \\ P_{in}^{s,j}, P_b^{s,j}}} \left\{ \beta_1 C_b + \beta_2 E_b + \sum_{s \in S} \sum_{j \in J} \rho_s \left(\lambda^j P_{in}^{s,j} \right) \right\} \quad (9a)$$

$$\text{s.t. } P_{in}^{s,j} + P_b^{s,j} + \hat{N}_{pv} P_{PV}^{s,j} \geq \sum_{k \in K} \hat{W}_k^j P_{ac,k} \quad (9b)$$

$$P_{\min} \leq P_{in}^{s,j} \leq P_{\max} \quad (9c)$$

$$0 \leq E_0 - \sum_{i=1}^j P_b^{s,i} \leq E_b \quad (9d)$$

$$-C_b \leq P_b^{s,j} \leq C_b \quad \forall s \in S, j \in J, k \in K \quad (9e)$$

In this step, the subproblem could be infeasible when the available power cannot meet the total demand. In this case, a

feasibility cut is generated and added to the master problem as follows:

$$\min_{Y, P_{in}^{s,j}, P_b^{s,j}} \mathbf{1}^T Y \quad (10a)$$

$$\text{s.t.} \quad P_{in}^{s,j} + P_b^{s,j} + Y^{s,j} \geq \sum_{k \in K} \hat{W}_k^j P_{ac,k} - \hat{N}_{pv} P_{PV}^{s,j} \quad (10b)$$

$$Y^{s,j} \geq 0, \forall s \in S, j \in J, k \in K$$

After generating a feasibility cut, $u_{r,j}^s$, the dual associated with this problem is taken. The general form of this cut is:

$$\sum_{s \in S} \sum_{j \in J} u_{r,j}^s \left(\sum_{k \in K} W_k^j P_{ac,k} - N_{pv} P_{PV}^{s,j} \right) \leq 0 \quad (11)$$

In the case where the problem is feasible, then the upper bound Z_{upper} is calculated and the convergence behavior is tested. If the convergence is not approached, then an optimality cut is generated and added to the master problem.

$$Z_{\text{upper}} = \left\{ \beta_1 \hat{C}_b + \beta_2 \hat{E}_b + \alpha \hat{N}_{pv} + \sum_{s \in S} \sum_{j \in J} \rho_s \left(\lambda^j \hat{P}_{in}^{s,j} \right) \right\} \quad (12)$$

We assume that $u_{p,j}^s$ are the dual variables associated with constraints (10b). Then the optimality cut is formed as the following

$$Z_{\text{lower}} \geq \alpha N_{pv} + \sum_{s \in S} \sum_{j \in J} u_{p,j}^s \left(P_{PV}^{s,j} N_{pv} + \sum_{k \in K} W_k^j P_{ac,k} \right). \quad (13)$$

c) *Step 3:* The master problem with the added constraints from Step 2 will be solved. The subproblem will again use the obtained optimal solutions for the integer variables from the master problem to solve and find the optimal solution for the other variables. The procedure keeps going until convergence is achieved by examining the low bound Z_{lower} and the upper bound Z_{upper} .

B. Benders Decomposition with Multiple Subproblems

The algorithm in the previous subsection separates the original problem into a master problem and a subproblem. In this subsection, we further explore the parallel computing structure of the problem and separate the original problem into a master problem with multiple subproblems.

The main philosophy here is to enable the subproblems to become decomposed over scenarios. Each subproblem is related to a stochastic scenario and the subproblems are independent once the main problem stage variables are determined.

The battery parameters C_b and E_b will be added to the set of the decision variables in the master problem. So the subproblem will only include the rest of the variables including battery power dispatch level and the purchased power for each scenario.

Step 1 In this step, we assume that power demand and all battery dispatched level are all zero. Only the HVAC operation

and the power and energy ratings of a battery are considered. The master problem is formed as follows.

$$\min_{C_b, E_b, N_{pv}, W_k^j} Z_{\text{lower}} \quad (14a)$$

$$\text{s.t.} \quad Z_{\text{lower}} \geq \alpha N_{pv} + \beta_1 C_b + \beta_2 E_b \quad (14b)$$

$$T_k^{j+1} = T_o^{j+1} + W_k^j QR - (T_o^{j+1} + W_k^j QR - T_k^j) e^{-\frac{\Delta t}{RC}} \quad (14c)$$

$$T_{\min} \leq T_k^{j+1} \leq T_{\max} \quad \forall j \in J, k \in K \quad (14c)$$

$$C_b, E_b \geq 0 \quad (14d)$$

Step 2 Form the independent subproblems and use the obtained optimal solution for the integer variables from the master problem ($\hat{N}_{pv}, \hat{W}_k^j, \hat{C}_b, \hat{E}_b$). Notice that each subproblem is solved independently. The formulation of a subproblem for a single scenario is given as follows.

$$\min_{P_{in}^{s,j}, P_b^{s,j}} \rho_s \sum_{j \in J} \left(\lambda^j P_{in}^{s,j} \right) \quad (15a)$$

$$\text{s.t.} \quad P_{in}^{s,j} + P_b^{s,j} + \hat{N}_{pv} P_{PV}^{s,j} \geq \sum_{k=1}^K \hat{W}_k^j P_{ac,k} \quad (15b)$$

$$P_{\min} \leq P_{in}^{s,j} \leq P_{\max} \quad (15c)$$

$$-\hat{C}_b \leq P_b^{s,j} \leq \hat{C}_b \quad (15d)$$

$$0 \leq E_0 - \sum_{i=1}^j P_b^{s,i} \leq \hat{E}_b, \quad (15e)$$

$$\forall s \in S, \forall j \in J, k \in K$$

Maximum Feasible Subsystem Cut Generation: For any infeasible subproblem, we would need to generate the feasibility cut from a maximum feasible subsystem [32]. This strategy makes cut generation highly effective when there are relatively large number of feasibility cuts. The strategy is to generate additional optimality cuts for the infeasible subproblems. This requires to first relax the infeasible subproblems. This technique has been used in [28] for individual stochastic scenarios.

For any infeasible subproblem of Scenario s , we will first relax the problem by finding a binary variable $Y^{s,j}$. If $Y^{s,j} = 0$, that means at j -th horizon the power balance is kept. $Y^{s,j} = 1$ means the power supply cannot meet the power demand.

$$\min_{Y^{s,j}, P_{in}^{s,j}, P_b^{s,j}} \sum_{j \in J} Y^{s,j} \quad (16a)$$

$$\text{s.t.} \quad P_{in}^j + P_b^j + Y^j M \geq \sum_{k \in K} \hat{W}_k^j P_{ac,k} - \hat{N}_{pv} P_{PV}^j$$

where $Y^{s,j}$ is a binary variable and M is a big number. Now, the obtained value $\hat{Y}^{s,j}$ is used to relax the infeasible subproblem.

$$\min_{P_{in}^{s,j}, P_b^{s,j}} \rho_s \sum_{j \in J} \left(\lambda^j P_{in}^{s,j} \right) \quad (17a)$$

$$\text{s.t.} \quad P_{in}^{s,j} + P_b^{s,j} + \hat{N}_{pv} P_{PV}^{s,j} + \hat{Y}^{s,j} M \geq \sum_{k \in K} \hat{W}_k^j P_{ac,k} \quad (17b)$$

$$P_{\min} \leq P_{in}^{s,j} \leq P_{\max} \quad (17c)$$

$$-\hat{C}_b \leq P_b^{s,j} \leq \hat{C}_b \quad (17d)$$

$$0 \leq E_0 - \sum_{i=1}^j P_b^{s,i} \leq \hat{E}_b, \quad (17e)$$

$$\forall s \in S, \forall j \in J, k \in K$$

With the optimal solution obtained, Z_{upper} is calculated by (18) and the convergence behavior is tested.

$$Z_{\text{upper}} = \left\{ \beta_1 \hat{C}_b + \beta_2 \hat{E}_b + \alpha \hat{N}_{pv} + \sum_{s \in S} \sum_{j \in J} \rho_s \left(\lambda^j \hat{P}_{in}^{s,j} \right) \right\} \quad (18)$$

If the convergence is not approached, then an optimality cut is generated and added to the master problem. To create the optimality cut, the dual variables must be extracted. The dual variables are $u_{p,j}^s$ associated with constraints (15b), (17b), $u_{C,j}^s$ associated with (15d), (17d), and $u_{E,j}^s$ associated with (15e), (17e).

The optimality cut is shown as follows.

$$Z_{\text{lower}} \geq \alpha N_{pv} + \sum_{s \in S} \sum_{j \in J} u_{p,j}^s \left(P_{PV}^{s,j} N_{pv} + \sum_{k \in K} W_k^j P_{ac,k} \right) + \left(\beta_1 + \sum_{s \in S} \sum_{j \in J} u_{C,j}^s \right) C_b + \left(\beta_2 + \sum_{s \in S} \sum_{j \in J} u_{E,j}^s \right) E_b \quad (19)$$

C. Benchmark of the algorithms

We first use a small-scale problem (3 scenarios, 30 binary decision variables, 318 continuous decision variables, and 257 equality constraints) to benchmark the two algorithms. The two Bender's decomposition algorithms are programmed and tested against the solution generated by CVX Gurobi. The results from the two algorithms exactly match the objective function result (13.7695) obtained from CVX Gurobi as shown in Fig. 3.

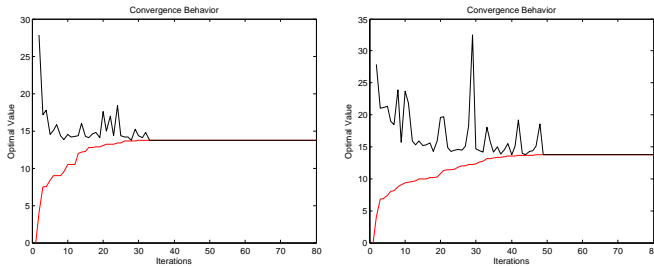


Fig. 3: (a). Lower and upper bounds of Strategy 1 for a small case; (b). Lower and upper bounds of Strategy 2 for a small case.

V. CASE STUDIES AND NUMERICAL EXAMPLES

A. The Study System

The study system shown in Fig. 4 consists of multiple PVs (each at 1.6 kW), one BESS, and three HVAC units (rated at 15 kW each) in their cooling modes. HVAC units

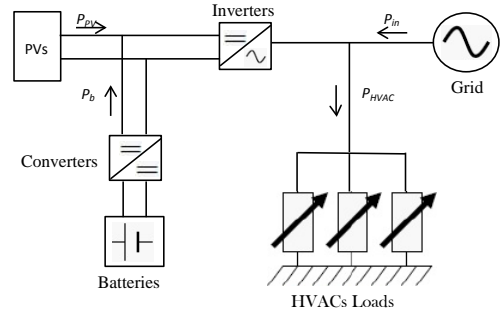


Fig. 4: The study system.

consume electricity from the grid at a varying price, shown in Fig. 5, during known periods. Room temperature should be maintained within a defined range by the consumer. Here, the consumer is to set thermostat point settings to 71 F as minimum limit and 75 F as maximum limit. The ambient temperature is shown in Fig. 5. The parameters C , R , and Q are shown in Table II.

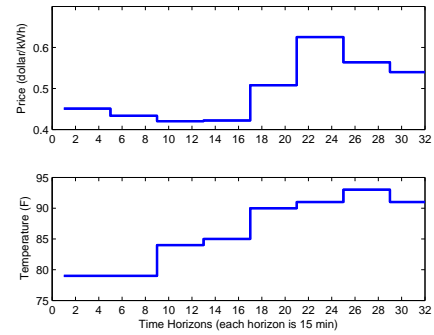


Fig. 5: Energy price and ambient temperature of 8 hours (32 periods).

TABLE II: Parameter values for HVAC units

	$Q(W)$	$R(F/W)$	$C(J/F)$
Values	400	0.1208	3599.3

B. Result and Analysis

We consider the system is connected to the grid and can purchase the power from the grid at a varying price. Three cases would be considered to study the effect of the uncertainty. The first case, Case-1, is used to study the behavior of the system without PV-BESS. In the second case Case-2, PV-BESS installation is considered in the deterministic mode to study the effect of solar energy. Two scenarios were studied. The first scenario, Case-2A, is assumed to have high availability of solar energy. The second scenario, Case-2B, is assumed to have poor availability of solar energy.

In the last two cases, stochastic MIP programming problem is considered. Benders decomposition strategy 1 is applied to deal with the uncertainty of solar power. 600 scenarios are

considered. In the fourth case, Case-4, 1500 scenarios are examined and the problem is solved using Benders decomposition strategy 2. Table III gives the parameters related to the cost function.

TABLE III: Cost Function Parameters

α	β_1	β_2
\$0.5/per panel	\$0.15 /kW	\$0.1 /kWh

The study results are presented in Table IV. It can be seen that the deterministic case with high availability of solar energy leads to the cheapest cost.

TABLE IV: Simulation Results

Case	BESS Capacity kWh	BESS Power kW	N_{pv}	Cost \$
Case-1	N/A	N/A	N/A	30.14
Case-2A	34.8	8.7	7	20.80
Case-2B	43.8	10.8	14	25.5
Case-3	37.6	9.40	7	22.32
Case-4	37.6	9.40	7	23.24

In Case-3 and Case-4, uncertainty of solar energy is considered. Case-3 and Case-4 lead to the almost same results with slight difference in cost. The difference is due to the consideration of more scenarios in Case-4.

Fig. 6(a) shows that the optimal value converges to \$22.32 when Benders decomposition Strategy-1 method is applied. Fig. 6(b) shows that the optimal value converged to \$23.24 when Benders decomposition Strategy-2 method applied.

Figs. 7–9 present results from Case-3. Fig. 7 presents the HVAC on/off schedule and the room temperature for one HVAC related to Case-3. Fig. 8 presents the numerical results related to two extreme scenarios that are among the 600 scenarios examined. Scenario 1 refers to the scenario when PV output is high while Scenario 2 refers to the scenario when PV output is low. Note that the total power consumed by three HVACs is limited to 15 kW. Fig. 9 further shows the switching status for every HVAC. We can find that minimizing operation cost makes sure that at one time, only one HVAC is turned on.

C. Computational Time

A program has been developed and implemented in MATLAB and solved using the CVX solver package and CPLEX. The numerical simulation has been performed on a 3.4-GHz based processor with 8GB of RAM.

Stochastic Mixed Integer Programming (SMIP) is developed to tackle the uncertainty. It is first solved as one original problem without any decomposition. The size of the problem increases as the number of scenarios increase. It includes a mixture of integer and continuous variables and would depend on the number of HVAC units, time horizons, and scenarios. This formulation is solved using CPLEX in MATLAB and the main challenge here is centered in the large number of the constraints of the power balance with integer variables.

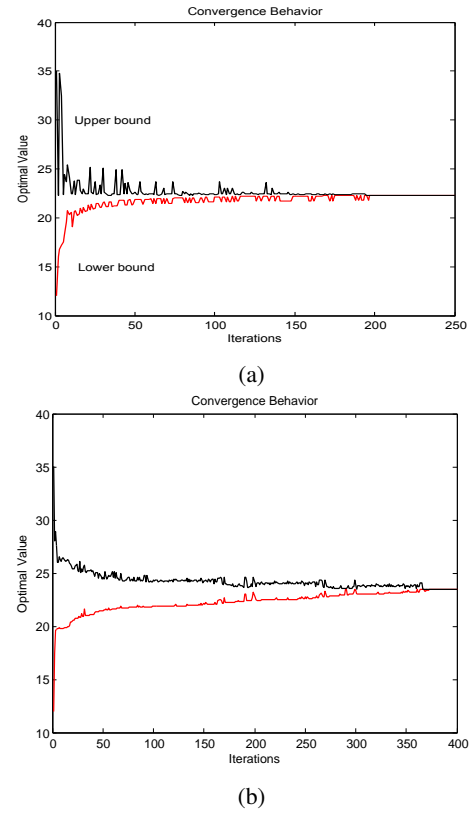


Fig. 6: (a) Lower and upper bound Strategy 1; (b) Lower and upper bound convergence of Strategy 2.

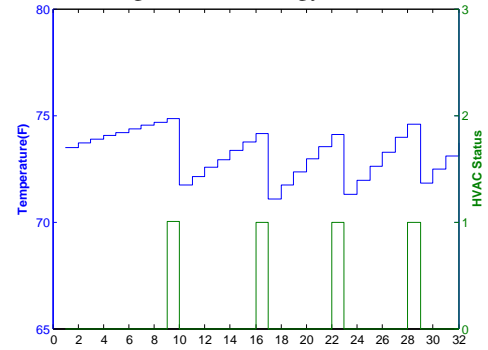


Fig. 7: HVAC on/off schedule and temperature.

Two Benders decomposition methods are also applied to solve the problem. A comparison of the three methods on problem size and computing time is shown in Table V.

Strategy 1: This problem is decomposed in a master problem and a subproblem. The size of the master problem is constant and it includes a mixture of integer and continuous variables and would depend on the number of HVAC units, and the time steps. When considering 3 HVAC and 32 time-steps, the problem would have 96 binary variables (related to 3 HVAC units running for 32-time steps) and one integer variable related to the number of PV. It would also have 99 continuous variables related to the room temperature. The size of the subproblem increases as the number of scenarios increase. It only includes continuous variables and would depend on the number of time-steps and the number of scenarios. In our case, we consider 32 time-steps and 600

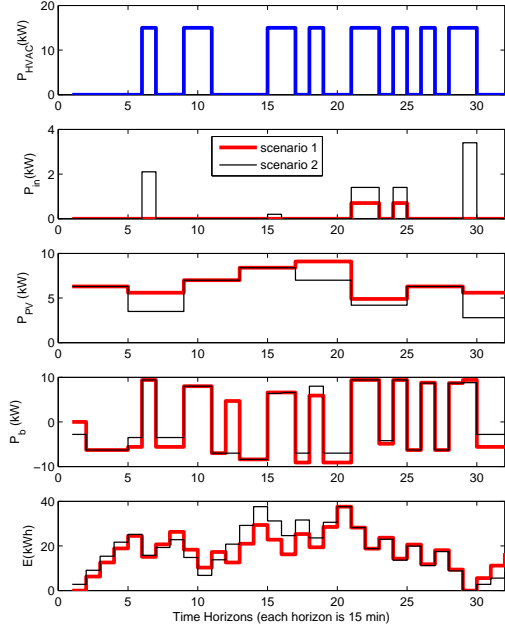


Fig. 8: Total HVAC power, purchased power, total PV output power, battery discharging power, and battery energy for two extreme scenarios.

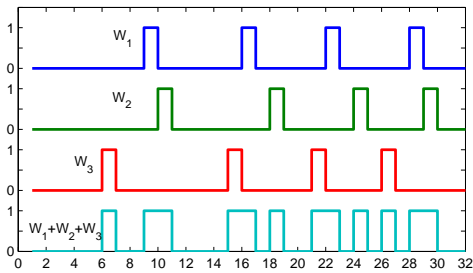


Fig. 9: Three HVAC on/off statuses: W_1 , W_2 , W_3 and $\sum W_k$.

scenarios. This would yield to 19200 continuous variables related to the purchased power considering 600 scenarios for 32-time steps and 19200 continuous variables related to battery power P_b . It also includes two continuous variables related to the Battery parameters (C_b and E_b).

This formulation is firstly solved using CVX for both the master and the sub problems. The advantage of CVX is its ability of returning dual variables along with primal variables. However, when the number of scenarios increases, CVX starts to have difficulty of solving. Therefore, a CPLEX formulation

TABLE V: Problem size and computing time

	Variables	CPLEX 18 scen.	CPLEX 600 scen.	Strategy 1 600 scen.	Strategy 2 1500 scen.
Original	Integer	97	97	97	97
	Cont.	1701	38501	38501	96101
Master	Integer	-	-	97	97
	Cont.	-	-	99	101
Sub	Integer	-	-	0	0
	Cont.	-	-	38402	96000
Time		390 m	> 24 h	35 m	150 m

is used for the master problem to tackle this challenge and CVX is used solving the subproblem. This strategy can work with a number of scenarios up to around 600. When the number of the scenarios increase, the size of the subproblem gets much larger and solving becomes more challenging.

Strategy 2 is different from Strategy 1 by moving the two continuous variables related to the Battery parameters (C_b and E_b) from the subproblem to the master problem. While in Strategy 1, the subproblem is considered as one whole problem including all variables, the subproblem in Strategy 2 is decomposed into multiple subproblems with each representing a scenario. This structure allows us to consider greater number of scenarios. Here, we are able to consider 1500 scenarios which would yield to have 48000 continuous variables related to the purchased power considering 1500 scenarios for 32-time steps and 48000 continuous variables related to battery power P_b . It also includes two continuous variables related to the Battery parameters (C_b and E_b). In this problem, the computing challenge is tackled by decomposing the subproblem in multiple subproblems. Strategy 2 shows the capability of handling 1500 scenarios while the Strategy 1 keeps running with no return when considering the same number of scenarios.

VI. CONCLUSION

This paper formulates the following engineering problem: planning battery and PV panels for a building with HVAC as the main loads. A mathematical programming problem is formulated to minimize the total installation cost as well the total energy cost purchased from utility. With PV's stochastic characteristic considered and HVAC treated as an on/off loads, the resulting mathematical programming problem is a large-scale mixed integer linear programming problem. This problem leads to the optimal size of the battery and number of PV panels required. To improve the solving speed for this decision making process, two Bender's decomposition formulations are proposed and used to solve the problem.

REFERENCES

- [1] A. Safdarian, M. Fotuhi-Firuzabad, and M. Lehtonen, "Benefits of demand response on operation of distribution networks: A case study," *IEEE systems journal*, vol. 10, no. 1, pp. 189–197, 2016.
- [2] [Online]. Available: <http://www1.eere.energy.gov/buildings/>
- [3] I. Beil, I. Hiskens, and S. Backhaus, "Frequency regulation from commercial building hvac demand response," *Proceedings of the IEEE*, vol. 104, no. 4, pp. 745–757, April 2016.
- [4] M. Muratori and G. Rizzoni, "Residential demand response: Dynamic energy management and time-varying electricity pricing," *IEEE Transactions on Power systems*, vol. 31, no. 2, pp. 1108–1117, 2016.
- [5] J. P. Barton and D. G. Infield, "Energy storage and its use with intermittent renewable energy," *IEEE Transactions on Energy Conversion*, vol. 19, no. 2, pp. 441–448, June 2004.
- [6] C. H. Lo and M. D. Anderson, "Economic dispatch and optimal sizing of battery energy storage systems in utility load-leveling operations," *IEEE Transactions on Energy Conversion*, vol. 14, no. 3, pp. 824–829, 1999.
- [7] A. Oudalov, D. Chartouni, and C. Ohler, "Optimizing a battery energy storage system for primary frequency control," *IEEE Transactions on Power Systems*, vol. 22, no. 3, pp. 1259–1266, 2007.
- [8] X. Y. Wang, D. M. Vilathgamuwa, and S. S. Choi, "Determination of battery storage capacity in energy buffer for wind farm," *IEEE Transactions on Energy Conversion*, vol. 23, no. 3, pp. 868–878, Sept 2008.

- [9] C. Abbey and G. Joós, “A stochastic optimization approach to rating of energy storage systems in wind-diesel isolated grids,” *IEEE Transactions on Power Systems*, vol. 24, no. 1, pp. 418–426, 2009.
- [10] P. Pinson, G. Papaefthymiou, B. Klockl, and J. Verboomen, “Dynamic sizing of energy storage for hedging wind power forecast uncertainty,” in *Power & Energy Society General Meeting, 2009. PES’09. IEEE*. IEEE, 2009, pp. 1–8.
- [11] S. Chakraborty, T. Senjyu, H. Toyama, A. Saber, and T. Funabashi, “Determination methodology for optimising the energy storage size for power system,” *IET generation, transmission & distribution*, vol. 3, no. 11, pp. 987–999, 2009.
- [12] Y. M. Atwa and E. El-Saadany, “Optimal allocation of ess in distribution systems with a high penetration of wind energy,” *IEEE Transactions on Power Systems*, vol. 25, no. 4, pp. 1815–1822, 2010.
- [13] Y. V. Makarov, P. Du, M. C. Kintner-Meyer, C. Jin, and H. F. Illian, “Sizing energy storage to accommodate high penetration of variable energy resources,” *IEEE Transactions on Sustainable Energy*, vol. 3, no. 1, pp. 34–40, 2012.
- [14] Y. Ma, F. Borrelli, B. Hency, B. Coffey, S. Bengea, and P. Haves, “Model predictive control for the operation of building cooling systems,” *IEEE Transactions on Control Systems Technology*, vol. 20, no. 3, pp. 796–803, May 2012.
- [15] Y. Ma, J. Matuko, and F. Borrelli, “Stochastic model predictive control for building hvac systems: Complexity and conservatism,” *IEEE Transactions on Control Systems Technology*, vol. 23, no. 1, pp. 101–116, Jan 2015.
- [16] P. Du and N. Lu, “Appliance commitment for household load scheduling,” *Smart Grid, IEEE Transactions on*, vol. 2, no. 2, pp. 411–419, 2011.
- [17] K. Zhou and L. Cai, “A dynamic water-filling method for real-time hvac load control based on model predictive control,” *IEEE Transactions on Power Systems*, vol. 30, no. 3, pp. 1405–1414, May 2015.
- [18] Z. Yu, L. Jia, M. C. Murphy-Hoye, A. Pratt, and L. Tong, “Modeling and stochastic control for home energy management,” *IEEE Transactions on Smart Grid*, vol. 4, no. 4, pp. 2244–2255, Dec 2013.
- [19] A. Arabali, M. Ghofrani, M. Etezadi-Amoli, M. S. Fadali, and Y. Baghzouz, “Genetic-algorithm-based optimization approach for energy management,” *Power Delivery, IEEE Transactions on*, vol. 28, no. 1, pp. 162–170, 2013.
- [20] Y. Du, L. Jiang, C. Duan, Y. Li, and J. S. Smith, “Energy consumption scheduling of hvac considering weather forecast error through distributionally robust approach,” *IEEE Transactions on Industrial Informatics*, vol. PP, no. 99, pp. 1–1, 2017.
- [21] M. Asensio, P. M. de Quevedo, G. Munoz-Delgado, and J. Contreras, “Joint distribution network and renewable energy expansion planning considering demand response and energy storage part i: Stochastic programming model,” *IEEE Transactions on Smart Grid*, 2016.
- [22] M. Shafie-khah and P. Siano, “A stochastic home energy management system considering satisfaction cost and response fatigue,” *IEEE Transactions on Industrial Informatics*, 2017.
- [23] CPLEX ILOG, “11.0 users manual,” *ILOG SA, Gentilly, France*, p. 32, 2007.
- [24] Gurobi and Optimization, “Gurobi optimizer reference manual,” *URL <http://www.gurobi.com>*, 2015.
- [25] G. E. Sand, “Modeling and solving real-time scheduling problems by stochastic integer programming,” *Computers and Chemical Engineering*, vol. 28, pp. 1087 – 1103, 2004.
- [26] J. Wang, M. Shahidehpour, and Z. Li, “Security-constrained unit commitment with volatile wind power generation,” *Power Systems, IEEE Transactions on*, vol. 23, no. 3, pp. 1319–1327, 2008.
- [27] W. Zhang, Y. Xu, Z. Dong, and K. P. Wong, “Robust security constrained-optimal power flow using multiple microgrids for corrective control of power systems under uncertainty,” *IEEE Transactions on Industrial Informatics*, vol. 13, no. 4, pp. 1704–1713, Aug 2017.
- [28] L. Kuznia, B. Zeng, G. Centeno, and Z. Miao, “Stochastic optimization for power system configuration with renewable energy in remote areas,” *Annals of Operations Research*, vol. 210, no. 1, pp. 411–432, 2013.
- [29] L. Fan. (2015) Tutorial on cutting plane methods for economic dispatch problems. [Online]. Available: http://power.eng.usf.edu/docs/papers/2015NAPS/cutting_NAPS15.pdf
- [30] M. Alhaider, L. Fan, and Z. Miao, “Benders decomposition for stochastic programming-based pv/battery/hvac planning,” in *2016 IEEE Power and Energy Society General Meeting (PESGM)*, July 2016, pp. 1–5.
- [31] M. J. Sanjari and H. Gooi, “Probabilistic forecast of pv power generation based on higher order markov chain,” *IEEE Transactions on Power Systems*, vol. 32, no. 4, pp. 2942–2952, 2017.
- [32] G. K. Saharidis and M. G. Ierapetritou, “Improving benders decomposition using maximum feasible subsystem (mfs) cut generation strategy,” *Computers & chemical engineering*, vol. 34, no. 8, pp. 1237–1245, 2010.